Targeting lung cancer initiating cells by all-trans retinoic acid-loaded lipid-PLGA nanoparticles with CD133 aptamers

YU ZHANG[1*], JUAN ZHAO[1*], JING SUN[2], LU HUANG[1] and QINGFENG LI[1]

[1]Department of Oncology, Xiangyang Central Hospital, Affiliated Hospital of Hubei University of Arts and Science, Xiangyang, Hubei 441000; [2]Department of Pharmacy, Second Military Medical University, Shanghai 200433, P.R. China

Received June 22, 2018; Accepted August 22, 2018

DOI: 10.3892/etm.2018.6762

Abstract. Lung cancer initiating cells represent a specific subpopulation of lung cancer cells, which significantly contribute to the initiation, metastasis and recurrence of lung cancer. CD133, initially considered a marker of stem cells, is now considered as a marker for lung cancer initiating cells. All-trans retinoic acid (RA) has been demonstrated to cause the differentiation, inhibition of proliferation, and apoptosis of cancer cells and cancer initiating cells. However, there have been no reports on the activity of RA against lung cancer initiating cells. In the present study, the activity of RA against lung cancer initiating cells was investigated by determining the cytotoxicity, and performing a tumorsphere assay and flow cytometry-based analysis. In addition, to promote the therapeutic effect of RA in $CD133^+$ lung cancer initiating cells, RA-loaded lipid poly(lactic-co-glycolic acid) (PLGA) nanoparticles with CD133 aptamers (RA-LPNPs-CD133) were developed. The activity of RA and RA-LPNPs-CD133 against lung cancer initiating cells was also investigated. RA-LPNPs-CD133 had a size of 129.9 nm, and exhibited sustained release of RA during the 144-h period. For the first time, to the best of our knowledge, the present study demonstrated that RA exerted potent activity towards $CD133^+$ lung cancer initiating cells. The results also showed that RA-LPNPs-CD133 efficiently and specifically promoted the delivery of RA to $CD133^+$ lung cancer initiating cells, exhibiting superior inhibitory effects against $CD133^+$ lung cancer initiating cells compared with non-targeted nanoparticles and RA. To the best of our knowledge, the present study is the first to report the promotion of RA delivery via nanoparticles to lung cancer initiating cells and achievement of a superior inhibitory effect against lung cancer initiating cells by the utilization of CD133 aptamers. Therefore, RA-LPNPs-CD133 represents a promising tool for the elimination of lung cancer initiating cells.

Correspondence to: Dr Qingfeng Li or Dr Lu Huang, Department of Oncology, Xiangyang Central Hospital, Affiliated Hospital of Hubei University of Arts and Science, 136 Jingzhou Street, Xiangyang, Hubei 441000, P.R. China
E-mail: 1iqfeng@163.com
E-mail: 3402947236@qq.com

*Contributed equally

Key words: lung cancer, cancer initiating cells, nanoparticles, CD133, aptamers

Introduction

Lung cancer, which originates from the lung, represents an aggressive and life-threatening type of cancer worldwide. In 2017, lung cancer was the primary cause of cancer-associated mortality in the USA (1). Similarly, in 2015, lung cancer was the primary cause of cancer-associated death in men aged >75 years in China (2). Therefore, development of a therapy for lung cancer is urgently required to improve human health. Although substantial achievements have been made in lung cancer therapy, treatment failure and decreased survival rates are often encountered, owing to progression, recurrence, metastasis and multi-drug resistance of lung cancer (3,4). Lung cancer initiating cells are a specific subpopulation of lung cancer cells, which contribute to the progression, recurrence, metastasis, and multi-drug resistance of lung cancer (3,4). Therefore, targeting and eliminating lung cancer initiating cells is likely to contribute to curing lung cancer from the origin.

CD133 is a marker for lung cancer initiating cells (5). Bertolini *et al* (6), showed that $CD133^+$ lung cancer cells isolated from lung cancer tissues showed significantly increased aggressive properties compared with their counterparts, $CD133^-$ lung cancer cells, as reflected by their increased proliferative, clonogenic and tumorigenic properties. All-trans retinoic acid (RA), an active metabolite of vitamin A under the family retinoid, is a promising drug that can cause the differentiation, proliferation inhibition and apoptosis of cancer cells in various types of cancer (7,8). An RA-based differentiation therapy is regarded as a significant advance in cancer therapy, and RA has become the first choice drug for the treatment of acute promyelocytic leukemia (APL) (7). RA has also been demonstrated to be effective in treating APL as an adjuvant (8). In addition, RA has shown therapeutic potential against cancer initiating cells in several types of cancer, including breast cancer (9-11).

Although RA has been reported to exert promising therapeutic effects against lung cancer in previous studies, there have been no reports on the therapeutic effect of RA on lung cancer initiating cells (12-14). Furthermore, the aqueous solubility of RA is poor, resulting in it being a less promising candidate drug with low bioavailability and poor therapeutic effect *in vivo* (9). It is known that nanoparticle-based strategies can markedly improve the bioavailability and therapeutic index of conventional therapeutics, by improving the solubility of poorly soluble drugs and providing targeted delivery of drugs (15-17). Several studies have developed RA-loaded nanoparticles to facilitate the preclinical application of RA in cancer therapy (9,18). In these studies, the solubility and bioavailability of RA were markedly increased, and the RA-loaded nanoparticles exhibited superior therapeutic efficacy against cancer compared with that of RA (9,18).

Lipid-polymer hybrid nanoparticles of biodegradable polymers and lipids represent superior candidate drug delivery systems, as they combine the advantages of liposomes and polymer nanoparticles (19,20). Liposomes feature superior biocompatibility, and easy modification of the hydrophilic polymer, and targeting molecules including aptamers (21,22). The advantages of polymer nanoparticles include controlled and sustained release, high drug loading and superior stability (19,20). Therefore, the advantages of lipid-polymer hybrid nanoparticles include superior biocompatibility and stability, easy modification, and controlled and sustained release (19).

To promote the efficacy of chemotherapy drugs to cancer cells, considerable interest has been paid to aptamer-targeted nanoparticles (21-23). It is well-known that aptamer-targeted nanoparticles have improved the therapeutic effect of chemotherapy in various types of cancer (24,25). As CD133 is generally accepted as a marker of lung cancer initiating cells, it was hypothesized in the present study that CD133 aptamers can be used to promote the delivery of RA-loaded nanoparticles to lung cancer initiating cells. The purpose of the present study was to target lung cancer initiating cells through the construction of RA-loaded lipid-PLGA nanoparticles with CD133 aptamers (RA-LPNPs-CD133).

Materials and methods

Culture of H446 and A549 lung cancer cell lines. H446 and A549 cells are two human lung cancer cell lines. These cells were purchased from American Type Culture Collection (Manassas, VA, USA) and maintained at 37˚C under 5% CO_2 in Roswell Park Memorial Institute 1640 (RMPI-1640) medium (HyClone; GE Healthcare Life Sciences, Logan, UT, USA). The RPMI-1640 medium was supplemented with 10% fetal bovine serum (FBS), streptomycin (100 μg/ml), and penicillin (100 U/ml). The cell culture medium containing 10% FBS was replaced at 3-4 day intervals to ensure the cell growth was optimal.

Reagents and kits. Poly(DL-lactide-co-glycolide) (PLGA) with a molar ratio of lactide:glycolide of 50:50 (40-75 kDa), polyvinyl alcohol (PVA; 30-70 kDa), RA and organic reagents were all purchased from Sigma-Aldrich; EMD Millipore (Billerica, MA, USA). The lipids, including [(1,2-distearoyl-sn-glycero-3-phosphoethanolamine-N-maleimide-polyethylene glycol-2000; DSPE-PEG-Mal, 1,2-dioleoyl-sn-glycero-3-phosphoethanolamine-N-carboxyfluorescein; PECF)], phosphatidylcholine, and cholesterol were purchased from Avanti Polar Lipids (Alabaster, AL, USA). The CD133 MicroBead kit was provided by Miltenyi Biotec, Inc. (Shanghai, China). The ultra-low attachment surface 6-well dishes were purchased from Corning Life Sciences (Tewksbury, MA, USA). R&D Systems, Inc. (Minneapolis, MN, USA) provided recombinant anti-human CD133 Alexa Fluor® 488-conjugated antibody (cat. no. FAB11331G). The synthesis of CD133 aptamers with the sequence of 5'-SH-CCCUCCUACAUAGGG-3' was performed by Ruibo Co., Ltd. (Guangzhou, China). The Pierce BCA Protein Assay kit, FBS, B27, epidermal growth factor (EGF), basic fibroblast growth factor (bFGF), insulin-transferrin-selenium (ITS), 4',6'-diamidino-2-phenylindole dihydrochloride (DAPI) and the cell dissociation reagent (StemPro® Accutase®) were purchased from Thermo Fisher Scientific, Inc. (Waltham, MA, USA).

Expression of CD133 in lung cancer cell lines. The flow cytometry-based approach was used to perform the analysis of CD133 in lung cancer cell lines. In short, the lung cancer cells were dissociated into single cells, and the dissociated cells were treated with the fluorescent antibody (anti-human CD133 Alexa Fluor® 488-conjugated antibody at 1 μg/ml) for 0.5 h at 4˚C. The cells were then washed three times with phosphate-buffered saline (PBS) to wash away unconjugated fluorescent antibody. At the end of the assay, the washed cells were suspended in PBS, and a FACSCalibur flow cytometer (FCM; BD Biosciences, Franklin Lakes, NJ, USA) was used to analyze the proportion of positively stained cells and the mean fluorescence intensity of the cells.

Magnetic cell sorting-based separation. As the expression of CD133 in lung cancer cell lines was low, magnetic cell sorting-based separation was performed to separate the $CD133^+$ cells from lung cancer cells according to the manufacturer's protocol provided with the CD133 MicroBead kit from Shanghai Miltenyi Biotec, Inc. Following separation, the FACSCalibur FCM was used to analyze the proportion of positively stained cells, as described above.

Formation of tumorspheres of lung cancer cells. Tumorsphere formation of the lung cancer cells was assessed to evaluate the self-renewal ability of the lung cancer initiating cells when the single cells were suspended in serum-free medium. In short, lung cancer cells suspended in stem cell medium were cultured in Corning® ultra-low attachment surface 6-well dishes. The density of the suspended cells was 5,000 cells/well, and the components of the stem cell medium included DMEM/F12, B27 (1x), ITS (1X), EGF and bFGF (both cytokines were at a concentration of 20 ng/ml). The cells were cultured in the stem cell medium for 7 days at 37˚C, following which the tumorspheres were counted under an Olympus CKX41 conventional light microscope. For the second-passage tumorspheres, those of the first passage were washed with PBS and dissociated with a cell dissociation reagent (StemPro® Accutase®), and then propagated.

Tumorigenicity of lung cancer cells in mice. The tumorigenicity assay was performed by the inoculation of lung cancer cells into male BALB/c nude mice (aged 4-5 weeks old, ~20 g; 6 per group; 240 mice in total). The mice were obtained from the Shanghai Experimental Animal Center (Shanghai, China). Following delivery of mice, the mice were raised in a clean environment without pathogens, and were acclimated for ~7 days. Animals were housed in separate cages (3-4 animals per cage) and maintained under a controlled atmosphere (humidity, 50±7%; temperature, 21±1˚C) and with a 12 h light/dark cycle. Mice were allowed free access to food and water. All animal procedures were performed in line with the regulations of the Animal Administrative Committee of the Second Military Medical University (Shanghai, China). In brief, $CD133^+$ and $CD133^-$ lung cancer cells were isolated using the magnetic bead-based approach. The collected cells were then mixed with BD Matrigel™. The mixture of cells ($2x10^7$-$2x10^4$/ml) and gel (0.2 ml per mouse) was implanted subcutaneously into the right flank of mice. The tumor formation was recorded during an observation period of 15 weeks.

Fabrication and characteristics of RA-loaded lipid-PLGA nanoparticles. The RA-loaded lipid-PLGA nanoparticles were fabricated as described below. In brief, 0.5 mg RA and 5 mg PLGA were completely dissolved in acetone to form an oil phase. The oil solution was injected into 2% PVA solution, followed by homogenization. The mini-emulsion was then poured into 0.2% PVA solution, and rapidly mixed for 6 h to remove remaining acetone by evaporation. Subsequently, the nanoparticles were recovered using ultracentrifugation (80,000 g) for 30 min at 25˚C. At the same time, a lipid film composed of phosphatidylcholine, DSPE-PEG-Mal and cholesterol (57:3:40 molar ratio) was formed in a round bottom flask with a vacuum rotary evaporator. When the lipid film was formed, the prepared nanoparticles were added to hydrate the film. A hand held extruder (Avanti Polar Lipids) with 200-nm membranes was used to extrude the obtained lipid-polymer suspension to produce small and homogeneous nanoparticles. The resultant lipid-polymer nanoparticles were washed by centrifugation at a speed of 3,000 x g for 30 min at 25˚C with Amicon centrifugal filters (MWCO 100 kDa) with distilled water. The CD133 aptamers with thiol groups were incubated with the nanoparticles (molar ratio of aptamers to DSPE-PEG-Mal of 1:2) for 6 h at room temperature, with the aim of conjugating the aptamers with thiol groups to nanoparticles. Subsequently, the unconjugated aptamers were removed using Amicon centrifugal filters [molecular weight cut-off (MWCO) 100 kDa]. Nontargeted nanoparticles were developed using the method described above but without the addition of aptamers. Blank nanoparticles were also developed using the method described above without the initial addition of RA. The fluorescent PECF-labeled nanoparticles were established in a similar manner but with 0.1% (molar ratio) of PECF added to the lipid film.

The nanoparticles were as follows: RA-loaded lipid-PLGA nanoparticles (RA-LPNPs); RA-loaded lipid-PLGA nanoparticles with CD133 aptamers (RA-LPNPs-CD133); blank lipid-PLGA nanoparticles with CD133 aptamers (LPNPs-CD133).

Aptamer conjugation efficiency of lipid-PLGA nanoparticles. The aptamer conjugation efficiency of the prepared nanoparticles was defined as the quantity of conjugated aptamers on the nanoparticles relative to the total quantity of added aptamers in the preparation procedure. A simple and rapid ultrafiltration-based approach was used to evaluate the aptamer conjugation efficiency of the prepared nanoparticles. Briefly, the aptamers were incubated with the nanoparticles, and the mixture of aptamers/nanoparticles was centrifuged with the Amicon centrifugal filters (MWCO 100 kDa) at 3,000 x g for 30 min at 25˚C to remove the unconjugated aptamers. The unconjugated aptamers were measured using UV at 260 nm. Finally, the aptamer conjugation efficiency of the nanoparticles was evaluated using the following equation: $(M_t-M_u)/M_t$, where M_t is the mass of total aptamers and M_U is the mass of unconjugated aptamers.

Size, ζ-potential, morphology and drug loading of lipid-PLGA nanoparticles. The particle size and ζ-potential were evaluated using a Zetasizer Nano ZS90 instrument (Malvern Instruments, Ltd., Malvern, UK), following the diluting 100 μl of nanoparticles in 1.9 ml of pure water. Furthermore, the morphology of the nanoparticles was investigated using transmission electron microscopy (TEM) with the Hitachi H-600 microscope (Hitachi, Ltd., Tokyo, Japan) as described below. The nanoparticles were negatively stained with 2% phosphotungstic acid and dried on mesh copper TEM grids. The nanoparticles were then observed under TEM. The RA encapsulation efficiency and loading of the nanoparticles were determined by reverse-phased high performance liquid chromatography (HPLC) with an ODS column (Diamonsil®; packing carriers: 5 μm; length and width: 250x4.6 mm). The nanoparticles (5 mg) were fully dissolved in 1 ml dichloromethane. The dichloromethane solution was evaporated in a vacuum evaporator and 10 ml methanol was added to form a clear solution sample for HPLC. The analysis was performed with the Agilent HPLC system (Agilent Technologies, Inc., Cotati, CA, USA). The mobile phase was acetic acid/acetonitrile/water (0.5/95/4.5, volume/volume), and the flow rate was fixed at 1.0 ml/min. The detection wavelength of RA was set at 350 nm.

RA release from nanoparticles. The release of RA from lipid-PLGA nanoparticles was evaluated as described below. First, the lipid-PLGA nanoparticles at a concentration of 1 mg/ml were suspended in PBS or PBS with 10% FBS in a centrifuge tube. The nanoparticles were then placed on an orbital shaker at 37˚C with gentle agitation at a speed of 80 x g. Subsequently, at different designated time points, the centrifuge tubes were centrifuged at 15,000 x g for 30 min at 25˚C. The supernatant was then removed from the centrifuge tubes, and measured by HPLC as described above. The cumulative RA release rate from the nanoparticles was calculated using the following formula: (M_i/M_t) x100%, where M_i is the mass of released RA, and M_t is the total mass of RA.

In vitro targeting of fluorescent nanoparticles to lung cancer cells. The *in vitro* targeting of fluorescent nanoparticles to lung cancer cells was evaluated by flow cytometry. Briefly, the lung cancer cells were isolated as described above, and were

then cultured on 12-well cell culture plates overnight at 37˚C. The density of lung cancer cells was $5x10^5$ cells per well. The medium was then replaced with a fresh medium containing PECF or PECF-labeled nanoparticles (1 μg/ml PECF). After 2 h at 37˚C, the cells were washed with PBS to remove unbound nanoparticles, and dissociated into single cells. The cells were suspended in PBS and analyzed using a FACSCalibur FCM.

Fluorescent immunohistochemistry. The lung cancer cells were isolated using the magnetic cell sorting-based separation method described above. Subsequently, the cells were seeded on coverslips in 12-well tissue culture plates overnight. The cells were seeded at a density of $5x10^5$ cells per well. Following overnight incubation, the medium was replaced with fresh cell medium containing PECF or PECF-labeled nanoparticles (1 μg/ml PECF). After 4 h, the cell medium was aspirated and removed, and the cells were washed with PBST (PBS containing 0.1% Tween-20) twice. Following washing with PBST, 4% paraformaldehyde was added to fix the cells for 20 min at 4˚C. The cells were then incubated with the nuclear staining reagent DAPI. Finally, the Carl Zeiss LSM510 confocal microscope (Carl Zeiss AG, Oberkochen, Germany) was used to visualize the immunofluorescence of the cells. The blue fluorescence of DAPI and the green fluorescence of PECF were observed and merged.

Cytotoxic effects of nanoparticles on lung cancer cell lines. The cytotoxic effects of nanoparticles were examined using the Cell Counting Kit-8 (CCK-8) assay. Briefly, the lung cancer cells were washed, trypsinized, and seeded at a density of $4x10^3$ cells/well in 96-well cell culture plates overnight. Following overnight incubation, the medium was replaced with a fresh medium containing RA or nanoparticles at a series of concentrations (0.04, 0.13, 0.41, 1.23, 3.7, 11.1, 33.3, 100.0, 300.0 and 900.0 μg/ml) at 37˚C. After 72 h, the medium was replaced with fresh medium. The cell viability was examined using the CCK-8 assay with a microplate reader (Multiskan MK3). Finally, the data was processed using GraphPad Prism 5.0 (GraphPad Software, Inc., La Jolla, CA, USA) to calculate the IC_{50} values.

Impact of nanoparticles on the proportion of lung cancer initiating cells. Tumorsphere formation and the proportion of $CD133^+$ cells were examined to evaluate the impact of nanoparticles on the proportion of lung cancer initiating cells in the lung cancer cell population. In brief, the lung cancer cells were washed, trypsinized into single cells, and inoculated overnight in 12-well cell culture plates. The density of lung cancer cells was $5x10^4$ cells per well. Following overnight incubation, the removal of old cell culture medium was performed by aspiration and washing with PBS. Following washing, the cells were treated with fresh medium dissolved with the nanoparticles (at a concentration equivalent to 15 μg/ml RA). After 24 h, removal of the old medium was performed by aspiration, and the cells were washed. Fresh medium was then added to the cells and incubated for 72 h. The cells were then washed and trypsinized to single cells, and the formation of tumorspheres measured as described in the above section. Alternatively, flow cytometry was performed to measure the percentage of $CD133^+$ cells of the trypsinized cells.

Statistical analysis. The differences between two groups was measured with Student's non-paired t-test, and the differences among three or more groups were measured by one-way analysis of variance, and Newman-Keuls post hoc test was used. $P<0.05$ was considered to indicate a statistically significant difference. All data are presented as the mean ± standard deviation, unless otherwise stated.

Results

Fabrication and characterization of lipid-PLGA nanoparticles. The RA-loaded lipid-PLGA nanoparticles were fabricated in two steps. In the first step, PLGA nanoparticles were initially developed using the emulsion/solvent evaporation approach. In the second step, the prepared PLGA nanoparticles were coated with lipid-based film to form the RA-loaded lipid-PLGA nanoparticles. Finally, the thiolated aptamers were conjugated to the lipid-PLGA nanoparticles via the reaction of sulfydryl groups on the aptamers with maleimide groups of the lipid-PLGA nanoparticles. The size, ζ-potential and drug loading of nanoparticles are shown in Table I. The RA-LPNPs, as nanoparticles without conjugated aptamers, had a small size of 123.8 nm. The conjugation of aptamers did not significantly alter the size of the nanoparticles, as reflected by the fact that the RA-LPNPs-CD133 and LPNPs-CD133 had sizes of 129.9 and 122.5 nm, respectively. The ζ-potential of the nanoparticles was negative at approximately-18 mV. The drug loading of RA-LPNPs and RA-LPNPs-CD133 was 10.2 and 9.8%, respectively. The encapsulation efficiency of RA-LPNPs and RA-LPNPs-CD133 was 82.2 and 83.2%, respectively. The conjugation efficiency of aptamers on RA-LPNPs-CD133 was 25%. The size distribution of the nanoparticles is shown in Fig. 1A. On being negatively stained with phosphotungstic acid, TEM showed that the RA-LPNPs and RA-LPNPs-CD133 were spherical in shape (Fig. 1B). The RA release assay, shown in Fig. 1C, indicated that all nanoparticles exhibited sustained release of RA during the 144-h period. The RA release of all nanoparticles was markedly higher in the PBS + serum (10% FBS) group, compared with that in the PBS group ($P<0.05$), indicating that serum destabilized the nanoparticles and facilitated the release of RA.

$CD133^+$ subpopulation of lung cancer cells exhibit properties of lung cancer initiating cells. The isolation of $CD133^+$ cells was performed using the CD133 MicroBead kit for cell sorting, and the results showed that a high percentage of $CD133^+$ cells (>99%) was obtained. Tumorsphere formation is a common approach to identify the self-renewal ability of cancer initiating cells (16). As shown in Fig. 2A, the tumorsphere number of $CD13^+$ H446 cells was significantly higher than that of $CD133^-$ H446 cells (1st passage: $P<0.01$; 2nd passage: $P<0.001$). In the A549 cells, similar results were achieved (1st passage: $P<0.01$; 2nd passage: $P<0.001$; Fig. 2B).

The *in vivo* tumorigenicity assay showed that $CD133^+$ cells had markedly enhanced capacity in terms of lung cancer formation compared with $CD133^-$ cells (Fig. 2C and D). Compared with the $CD133^-$ cells, the tumor volume derived from $CD133^+$ cells was significantly larger at day 28 for the H446 cells and at day 24 for the A549 cells ($P<0.05$). The tumorigenicity in

Table I. Characteristics of nanoparticles.

Nanoparticle	Size (nm)	ζ-potential (mv)	PDI	Drug loading (%)	EE (%)
RA-LPNPs	123.8±15.2	-18.8±5.6	0.14±0.04	10.2±4.8	82.2±6.5
RA-LPNPs-CD133	129.9±13.2	-19.7±5.5	0.15±0.05	9.8±5.9	83.2±9.4
LPNPs-CD133	122.5±16.6	-17.3±4.9	0.16±0.07	-	-

Data are expressed as the mean ± standard deviation (n=4). PDI, polydispersity index; EE, encapsulation efficacy; RA-LPNPs, retinoic acid-encapsulated lipid-PLGA nanoparticles; RA-LPNPs-CD133, RA-LPNPs with CD133 aptamers; LPNPs-CD133, blank lipid-PLGA nanoparticles with CD133 aptamers.

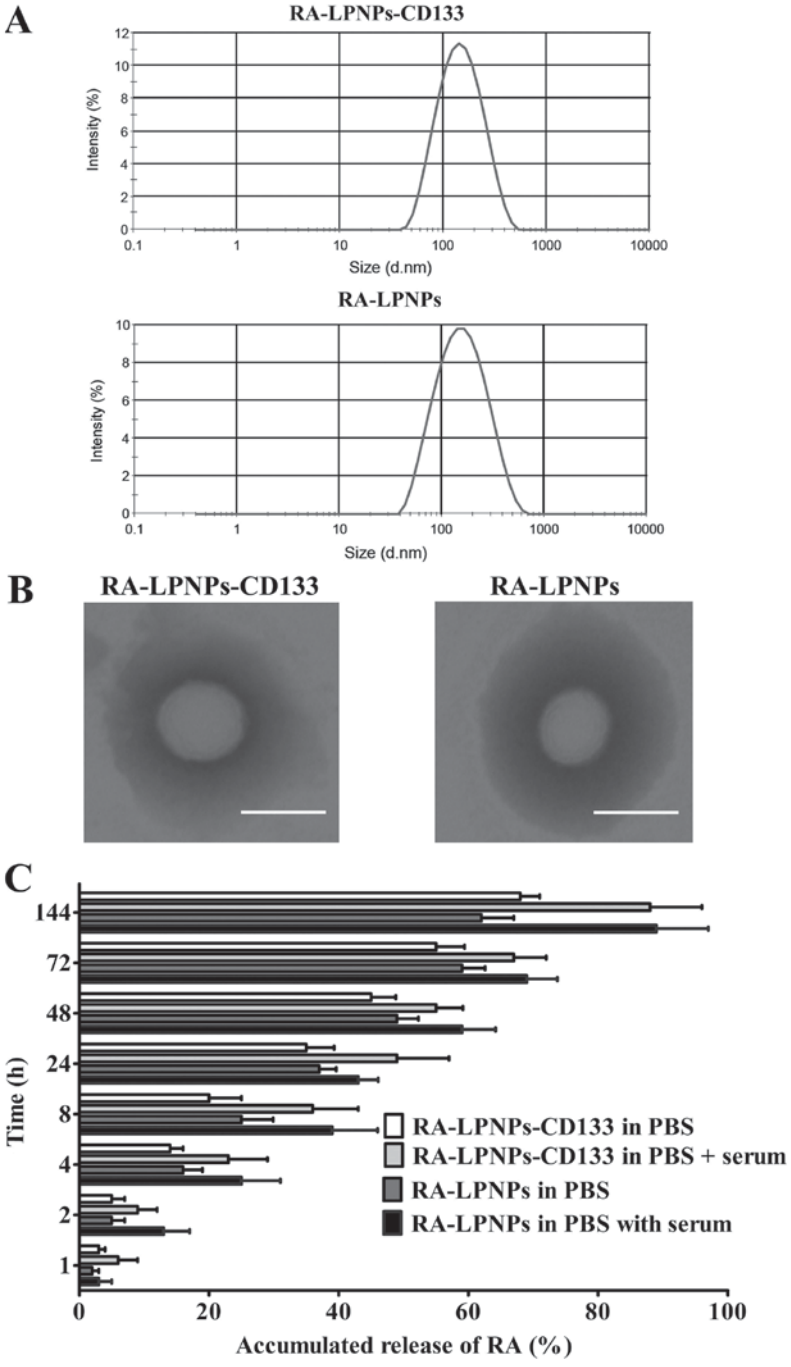

Figure 1. Characteristics of lipid-PLGA nanoparticles. (A) Size distribution of lipid-PLGA nanoparticles examined by the Zetasizer Nano ZS90 instrument. (B) Transmission electron microscopy images of nanoparticles stained with phosphotungstic acid. Scale bar=100 nm. (C) Accumulated release of RA from nanoparticles. The release media were PBS and PBS + serum (10% fetal bovine serum). Student's non-paired t-test was used to detect the difference between two groups. Data are presented as the mean ± standard deviation (n=3). RA, retinoic acid; LPNPs, lipid poly(lactic-co-glycolic acid); PBS, phosphate-buffered saline.

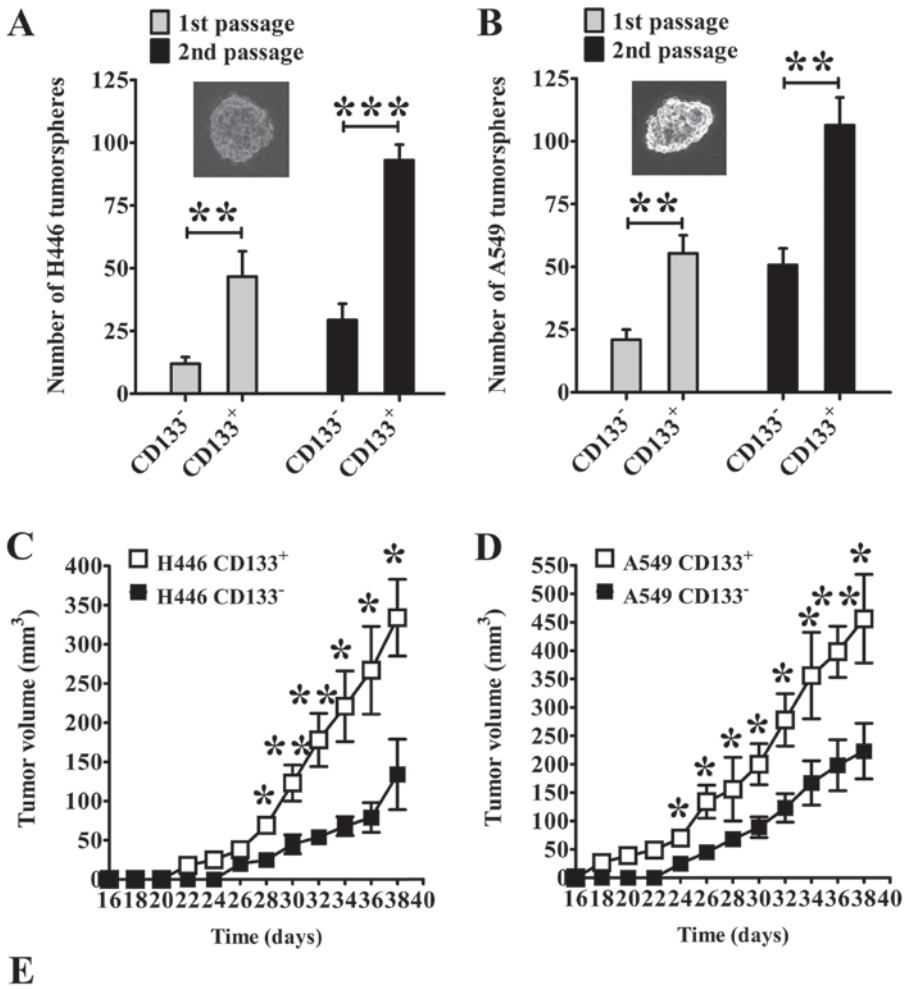

E

Types	2×10^6	2×10^5	2×10^4	1×10^4	5×10^3	2×10^3
$CD133^-$ H466	5/10	2/10	1/10	1/10	1/10	0/10
$CD133^+$ H466	10/10	10/10	10/10	9/10	8/10	5/10
$CD133^-$ A549	6/10	4/10	2/10	1/10	1/10	0/10
$CD133^+$ A549	10/10	10/10	10/10	9/10	7/10	3/10

Figure 2. $CD133^+$ lung cancer cells have properties of lung cancer initiating cells. Tumorsphere formation of (A) H446 and (B) A549 lung cancer cells. Representative images of tumorspheres are shown (magnification, x200). Data are presented as the mean ± standard deviation (n=6). Growth curves of (C) H446 and (D) A549 lung cancer cells in nude mice ($2x10^5$ lung cancer cells were implanted into the nude mice). Data are presented as the mean ± standard deviation (n=6). $^*P<0.05$; $^{**}P<0.01$; $^{***}P<0.001$. The two groups were compared using Student's non-paired t-test. (E) Tumorigenicity assay of lung cancer cells in mice.

mice also showed that $CD133^+$ cells had markedly enhanced capacity in terms of lung cancer formation (Fig. 2E). Notably, a 100% incidence of tumors (10/10) in mice was found in $CD133^+$ H446 cells with a cell count $\geq 2x10^4$ cells. By contrast, only a 60% incidence of tumors (6/10) in mice was found in $CD133^-$ H446 cells, even the cell number was $2x10^6$, indicating that $CD133^+$ H446 cells had significantly increased tumorigenic potential in comparison with $CD133^-$ H446 cells. Similarly, $CD133^+$ A549 cells had significantly increased tumorigenic ability in comparison with $CD133^-$ A549 cells. The $CD133^+$ A549 cells produced tumors in mice with a 100% incidence when the cell number was $\geq 2x10^4$ cells, whereas $CD133^-$ A549 cells only produced tumors with a 20% incidence (2/10) at $2x10^4$ $CD133^-$ A549 cells. Taken together, the tumorigenicity of $CD133^+$ lung cancer cells was markedly higher than that of $CD133^-$ lung cancer cells.

In vitro targeting and uptake of fluorescent nanoparticles in lung cancer cells. The green fluorescent lipid, PECF, is widely used in the evaluation of the cellular uptake of nanoparticles. As shown in Fig. 3A, the uptake of PECF-labeled RA-LPNPs-CD133 in the H446 $CD133^+$ cells was prominently higher compared with that of PECF ($P<0.001$) and PECF-labeled RA-LPNPs ($P<0.05$). However, in the H446 $CD133^-$ cells, uptake of PECF-labeled RA-LPNPs-CD133 was similar to that of PECF-labeled RA-LPNPs, although uptake was increased compared with that of free PECF ($P<0.05$). For the A549 cells, similar results were observed (Fig. 3B). The

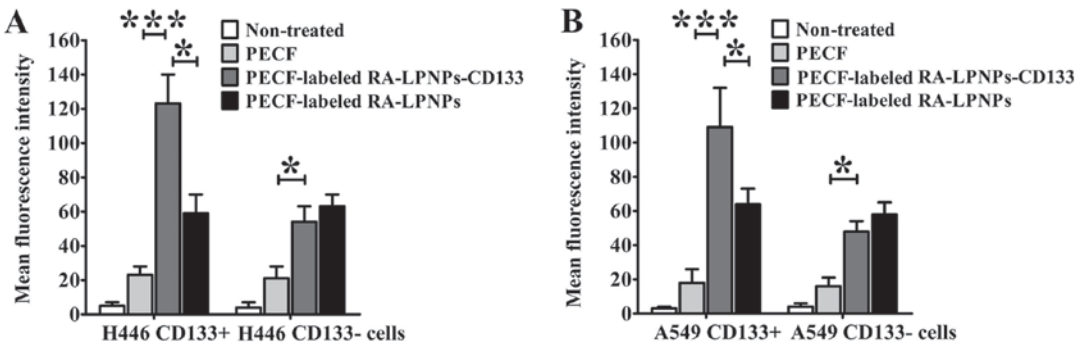

Figure 3. *In vitro* targeting of nanoparticles to lung cancer cells. (A) H446 cells; (B) A549 cells. One-way analysis of variance with the Newman-Keuls post hoc test was used to detect the difference between the two groups. Data are presented as the mean ± standard deviation (n=3). *P<0.05; ***P<0.001. RA, retinoic acid; LPNPs, lipid poly(lactic-co-glycolic acid); PECF, 1,2-dioleoyl-sn-glycero-3-phosphoethanolamine-N-(carboxyfluorescein).

PECF-labeled RA-LPNPs-CD133 showed increased uptake compared with the PECF-labeled RA-LPNPs (P<0.05) and free PECF (P<0.001) in the A549 CD133^{+} cells, with similar uptake of PECF-labeled RA-LPNPs in A549 CD133^{-} cells.

The *in vitro* cellular uptake of PECF-labeled nanoparticles was also evaluated by confocal microscopy. As shown in Fig. 4, H446 CD133^{+} cells treated with PECF labeled RA-LPNPs-CD133 showed significant internalization of nanoparticles. By contrast, non-targeted PECF-labeled RA-LPNPs showed no significant internalization in H446 CD133^{+} cells, as reflected by the reduced green fluorescence intensity compared with PECF-labeled RA-LPNPs-CD133. As expected, PECF exhibited the lowest green fluorescence intensity, suggesting that nanoparticles markedly facilitated the uptake of free drugs. In the H446 CD133^{-} cells, PECF-labeled RA-LPNPs-CD133 did not differ in green fluorescence intensity from PECF-labeled RA-LPNPs. Similar results were obtained in A549 cells. Taken together, PECF-labeled RA-LPNPs-CD133 showed specific increased uptake in CD133^{+} lung cancer cells.

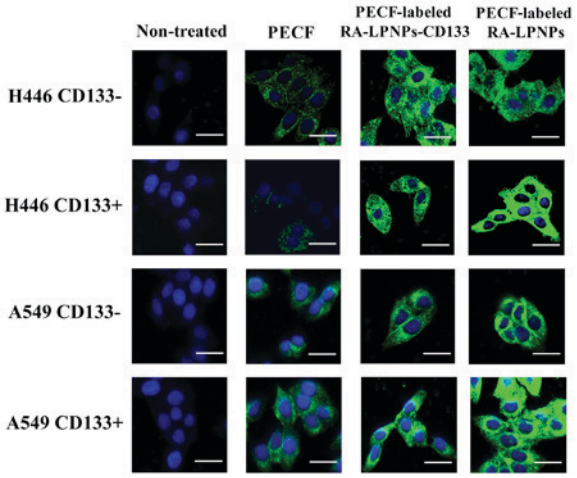

Figure 4. Fluorescent immunohistochemistry. CD133^{+} or CD133^{-} lung cancer cells (H446 and A549) were incubated with free PECF or PECF-labeled nanoparticles (1 μg/ml PECF). Cells were stained using DAPI. A confocal microscope was used to visualize the immunofluorescence of the cells. The blue fluorescence (represents DAPI) and green fluorescence (represents PECF) were observed. Scale bar=20 μm. RA, retinoic acid; LPNPs, lipid poly(lactic-co-glycolic acid); PECF, 1,2-dioleoyl-sn-glycero-3-phosphoethanolamine-N-(carboxyfluorescein); DAPI, 4',6'-diamidino-2-phenylindole dihydrochloride.

Cytotoxic effects of RA and various nanoparticles against lung cancer cells. As shown in Fig. 5A-D, LPNPs-CD133, the blank lipid-PLGA nanoparticles with CD133 aptamers, exhibited no marked cytotoxic effects towards lung cancer cells, as reflected by the almost horizontal curve induced by LPNPs-CD133. By contrast, dose-dependent cytotoxicity was observed for RA, RA-LPNPs and RA-LPNPs-CD133, as reflected by their dose-dependent curves of inverse sigmoid. The IC_{50} values of the RA and other nanoparticles are listed in Fig. 5E. In the CD133^{+} H446 cells, RA-LPNPs exhibited similar cytotoxic effect as RA (21.7 μg/ml for RA-LPNPs, vs. 18.2 μg/ml for RA). Compared with RA-LPNPs and RA, RA-LPNPs-CD133 possessed significantly increased cytotoxic effects (5.5 μg/ml) (P<0.001). However, the IC_{50} of RA-LPNPs-CD133 (49.7 μg/ml), RA-LPNPs (51.5 μg/ml) and RA (52.5 μg/ml) did not differ markedly in the CD133^{-} H446 cells. For the A549 cells, similar results were observed. In the CD133^{+} A549 cells, the cytotoxic effect of RA-LPNPs-CD133 (IC_{50} 8.5 μg/ml) was also markedly higher compared with that in other groups, including RA-LPNPs (28.5 μg/ml) and RA (29.9 μg/ml) (P<0.001), whereas its cytotoxic effect (65.7 μg/ml) in CD133^{-} A549 cells was similar to RA-LPNPs (65.5 μg/ml) and RA (57.5 μg/ml). Taken together, RA-LPNPs-CD133 exhibited preferential cytotoxic effects towards CD133^{+} lung cancer cells.

Impact of nanoparticles on lung cancer initiating cells. The impact of nanoparticles on the percentage of lung cancer initiating cells was investigated in the H446 and A549 lung cancer cell lines (Fig. 6A and B). In the H446 cells, treatment with RA markedly inhibited the number of tumorspheres (P<0.05; Fig. 6C). The inhibitory effect of RA was similar to that of RA-LPNPs, as reflected by their equal effects on the inhibition of tumorsphere formation. Notably, the number of tumorspheres following RA-LPNPs-CD133 treatment was significantly decreased compared with that following treatment with RA and RA-LPNPs (P<0.05). Treatment with LPNPs-CD133 had no effect on the number of tumorspheres. Similar results were observed in the A549 cells (Fig. 6D). Although the number of tumorspheres was not affected by treatment with LPNPs-CD133, treatment with RA-LPNPs-CD133 exhibited the most marked inhibitory activity on the number

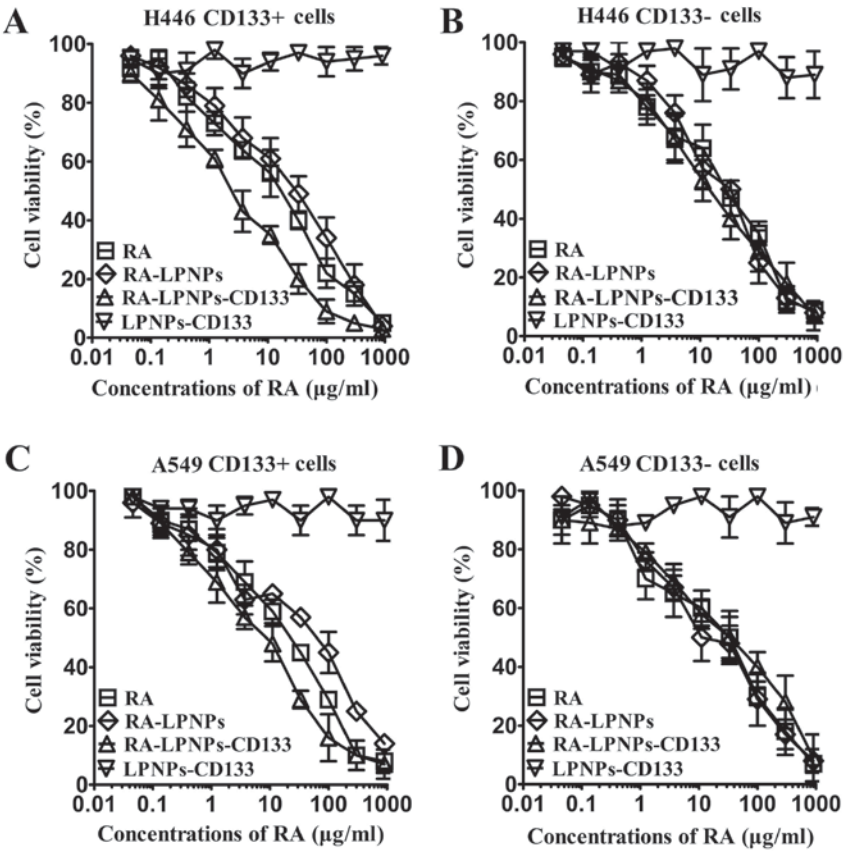

E

IC_{50} (μg/ml)	H446		A549	
	$CD133^+$	$CD133^-$	$CD133^+$	$CD133^-$
RA	18.2 ± 5.7	52.5 ± 9.4	29.9 ± 7.7	57.5 ± 9.3
RA-LPNPs	21.7 ± 6.7	51.5 ± 11.3	28.5 ± 7.6	65.5 ± 8.5
RA-LPNPs-CD133	5.5 ± 2.1	49.7 ± 9.9	8.5 ± 3.5	65.7 ± 7.8
LPNPs-CD133	> 900.0	> 900.0	> 900.0	> 900.0

Figure 5. Assessment of the cytotoxicity of nanoparticles towards lung cancer cells by Cell Counting Kit-8 assay. (A) Curves of nanoparticles in H446 $CD133^+$ cells; (B) curves of nanoparticles in H446 $CD133^-$ cells; (C) curves of nanoparticles in A549 $CD133^+$ cells; (D) curves of nanoparticles in A549 $CD133^-$ cells. (E) Cytotoxic effects of RA and nanoparticles as reflected by IC_{50} values in lung cancer cells at 72 h. Data are presented as the mean ± standard deviation (n=3). RA, retinoic acid; LPNPs, lipid poly(lactic-co-glycolic acid).

of tumorspheres in A549 cells. Consistent with the above results, the percentage of $CD133^+$ H446 cells was significantly reduced following RA treatment ($P<0.05$; Fig. 7A). RA and RA-LPNPs exhibited similar inhibitory effects towards the percentage of $CD133^+$ H446 cells. The percentage of $CD133^+$ H446 cells was the lowest among all groups following treatment with RA-LPNPs-CD133. As shown in Fig. 7B, similar results were obtained in the case of A549 cells. Taken together, RA-LPNPs-CD133 exhibited the optimal efficacy towards lung cancer initiating cells.

Discussion

Lung cancer initiating cells are regarded as the initial cause of lung cancer. Therefore, the eradication of lung cancer initiating cells is considered an effective treatment. CD133 is a marker of lung cancer initiating cells. In the present study, RA-loaded lipid-PLGA nanoparticles conjugated with CD133 aptamers, RA-LPNPs-CD133, were constructed to target lung cancer initiating cells. RA-LPNPs-CD133 exhibited significantly higher therapeutic effects towards lung cancer initiating cells than did free RA and non-targeted nanoparticles.

Nanoparticles of biodegradable polymers represent superior drug delivery systems. Their advantages include controlled and sustained release, high drug loading capacity and superior stability (24). Lipid-PLGA nanoparticles represent one of the most commonly used nanoparticles of biodegradable polymers, due to their superior biocompatibility and flexibility in modulation of drug release (19).

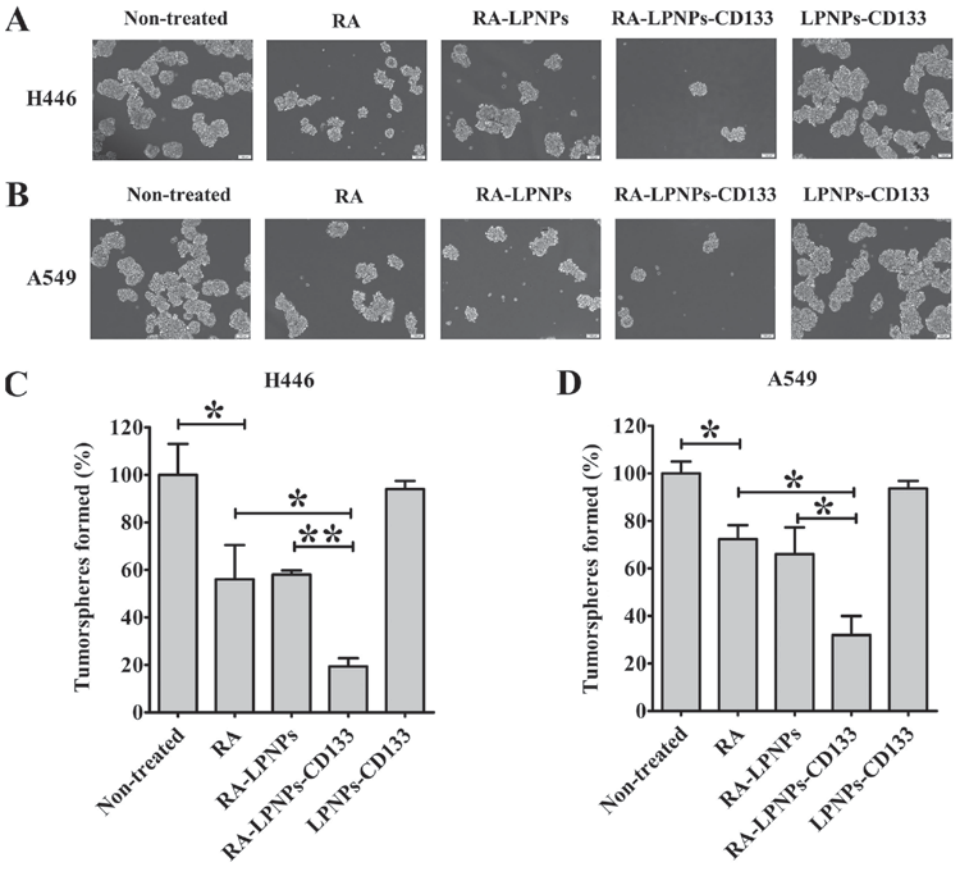

Figure 6. Impact of nanoparticles on the percentages of lung cancer initiating cells. The experiment involved evaluation of the tumorsphere formation assay. Representative images of tumorspheres in (A) H446 and (B) A549 cells are shown. Quantitative analysis of the tumorspheres in (C) H446 and (D) A549 cells. Data are presented as the mean ± standard deviation (n=6). *P<0.05; **P<0.01. Scale bars, 100 μm. RA, retinoic acid; LPNPs, lipid poly(lactic-co-glycolic acid).

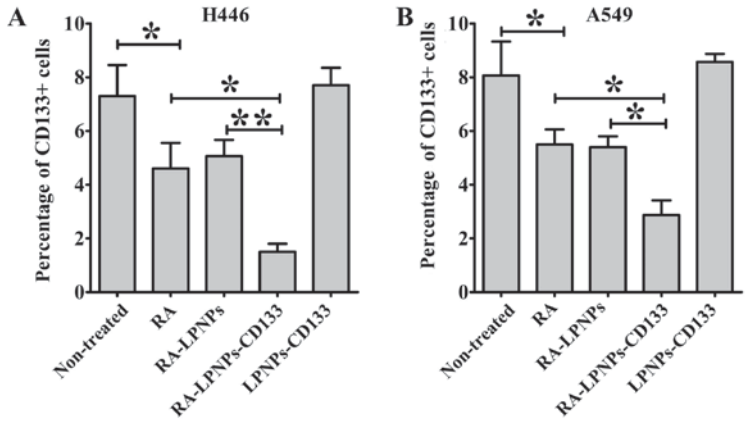

Figure 7. Impact of nanoparticles on the percentages of lung cancer initiating cells. The experiment involved the evaluation of the percentage of CD133^{+} cells in (A) H446 and (B) A549 cells. Data are presented as the mean ± standard deviation (n=6). *P<0.05; **P<0.01. RA, retinoic acid; LPNPs, lipid poly(lactic-co-glycolic acid).

Commonly, poly(ethylene glycol) (PEG) chains can be incorporated as copolymers throughout the nanoparticles to increase the hydrophilicity, modification flexibility and circulation time of the nanoparticles (20). However, PEGylation of PLGA nanoparticles requires the synthesis of PLGA-PEG copolymers. In preparing lipid-PLGA nanoparticles in the present study, the DSPE-PEG molecule was inserted into the nanoparticles by physical mixing, avoiding the complicated synthesis of PLGA-PEG copolymers. Furthermore, unlike biodegradable organic nanoparticles, inorganic nanoparticles cannot be degraded, and may cause damage to humans (26,27). Therefore, the potential clinical use of inorganic nanoparticles is limited by their poor safety (27). By contrast, biodegradable organic nanoparticles are more promising in clinical application due to their superior safety profile (26,27). In the present study, the components of RA-LPNPs-CD133 included lipids, PLGA and a CD133 antibody, which are safe USA Food and Drug Administration (FDA)-approved biomaterials. As for

RA, the FDA has approved the combination use of arsenic trioxide (Trisenox) injection plus RA, as a first-line treatment for low-risk acute promyelocytic leukemia. In the present study, LPNPs-CD133, comprising blank lipid-PLGA nanoparticles with CD133 aptamers, exhibited no marked cytotoxic effects towards lung cancer cells, as reflected by the almost horizontal curve induced by LPNPs-CD133. The preliminary safety data in the present study demonstrated that the nanoparticles represent a safe drug delivery system. Therefore, CD133-SA-NP is expected to be safe in clinic use, and this safety is likely to facilitate its clinical translation.

RA is a promising drug that has shown potential therapeutic effects in various types of cancer, including bladder cancer (7). Its anticancer mechanisms include promising effects on the growth, differentiation and apoptosis of cancer cells (7,8). It is noteworthy that RA has shown therapeutic potential against cancer initiating cells in several types of cancer (9-11). To the best of our knowledge, there have been no reports on the therapeutic effect of RA on lung cancer initiating cells. In the present study, it was confirmed that RA preferentially eliminated $CD133^+$ lung cancer initiating cells. In the tumorsphere formation assay, RA also reduced the tumorsphere numbers in lung cancer cells. Consistently, the percentage of $CD133^+$ cells in lung cancer cells was significantly decreased following RA treatment. To the best of our knowledge, the present study is the first to demonstrate that RA exhibits potential activity towards lung cancer initiating cells.

Ligand-conjugated nanoparticles are a promising tool against various types of cancer, as they can significantly enhance the therapeutic efficacy of chemotherapy drugs (21-23). Notably, three types of ligand-conjugated nanoparticles have been successfully translated into early-phase clinical trials (28,29). In the present study, the selection of CD133 aptamers was critical for the specific targeting of the developed nanoparticles to lung cancer initiating cells. The results showed that, in $CD133^+$ lung cancer initiating cells, RA-LPNPs-CD133 exhibited significantly increased targeting compared with RA-LPNPs, resulting in increased cytotoxic effects and inhibitory effects on tumorspheres. However, in $CD133^-$ lung cancer cells, the cytotoxicity and tumorsphere inhibitory effects of RA-LPNPs-CD133 did not differ from those of RA-LPNPs. These data firmly demonstrated that RA-LPNPs-CD133 was able to exert increased targeting and therapeutic effects towards lung cancer initiating cells and that CD133 aptamers promoted the targeting of nanoparticles to lung cancer initiating cells. To the best of our knowledge, the present study is the first to report the promotion of RA delivery via nanoparticles to lung cancer initiating cells by the utilization of CD133 aptamers.

In conclusion, the present study provides the first report of the anticancer activity of RA against lung cancer initiating cells. RA-LPNPs-CD133 selectively targeted $CD133^+$ lung cancer initiating cells. Therefore, RA-LPNPs-CD133 represents a promising approach for therapy targeting lung cancer initiating cells.

Acknowledgements

Not applicable.

Funding

The present study was supported by the Xiangyang Municipal Fund (grant no. 20140915).

Authors' contributions

QL and LH contributed to the design of the study and wrote the manuscript. YZ and JZ performed the experiments. JS analyzed the data. All authors have read and approved the manuscript.

Availability of data and materials

All data generated or analyzed during the present study are included in the published article.

Ethics approval and consent to participate

The animal experimental protocols were approved by the Animal Administrative Committee of the Second Military Medical University (Shanghai, China).

Patient consent for publication

Not applicable.

Authors' information

YZ, JZ, LH and QL: Department of Oncology, Xiangyang Central Hospital, Affiliated Hospital of Hubei University of Arts and Science, 136 Jingzhou Street, Xiangyang, Hubei 441000, P.R. China; JS: Department of Pharmacy, The Second Military Medical University, 325 Guohe Road, Shanghai 200433, P.R. China.

Competing interests

The authors declare that they have no competing interests.

References

1. Siegel RL, Miller KD and Jemal A: Cancer statistics, 2017. CA Cancer J Clin 67: 7-30, 2017.
2. Chen W, Zheng R, Baade PD, Zhang S, Zeng H, Bray F, Jemal A, Yu XQ and He J: Cancer statistics in China, 2015. CA Cancer J Clin 66: 115-132, 2016.
3. Eramo A, Lotti F, Sette G, Pilozzi E, Biffoni M, Di Virgilio A, Conticello C, Ruco L, Peschle C and De Maria R: Identification and expansion of the tumorigenic lung cancer stem cell population. Cell Death Differ 15: 504-514, 2008.
4. Kim JJ and Tannock IF: Repopulation of cancer cells during therapy: An important cause of treatment failure. Nat Rev Cancer 5: 516-525, 2005.
5. Zakaria N, Satar NA, Abu Halim NH, Ngalim SH, Yusoff NM, Lin J and Yahaya BH: Targeting lung cancer stem cells: Research and clinical impacts. Front Oncol 7: 80, 2017.
6. Bertolini G, Roz L, Perego P, Tortoreto M, Fontanella E, Gatti L, Pratesi G, Fabbri A, Andriani F, Tinelli S, *et al*: Highly tumorigenic lung cancer CD133+ cells display stem-like features and are spared by cisplatin treatment. Proc Natl Acad Sci USA 106: 16281-16286, 2009.
7. Siddikuzzaman, Guruvayoorappan C and Berlin Grace VM: All trans retinoic acid and cancer. Immunopharmacol Immunotoxicol 33: 241-249, 2011.

8. Montesinos P, Bergua JM, Vellenga E, Rayón C, Parody R, de la Serna J, León A, Esteve J, Milone G, Debén G, *et al*: Differentiation syndrome in patients with acute promyelocytic leukemia treated with all-trans retinoic acid and anthracycline chemotherapy: Characteristics, outcome, and prognostic factors. Blood 113: 775-783, 2009.
9. Li RJ, Ying X, Zhang Y, Ju RJ, Wang XX, Yao HJ, Men Y, Tian W, Yu Y, Zhang L, *et al*: All-trans retinoic acid stealth liposomes prevent the relapse of breast cancer arising from the cancer stem cells. J Control Release 149: 281-291, 2011.
10. Karsy M, Albert L, Tobias ME, Murali R and Jhanwar-Uniyal M: All-trans retinoic acid modulates cancer stem cells of glioblastoma multiforme in an MAPK-dependent manner. Anticancer Res 30: 4915-4920, 2010.
11. Han D, Rodriguez-Bravo V, Charytonowicz E, Demicco E, Domingo-Domenech J, Maki RG and Cordon-Cardo C: Targeting sarcoma tumor-initiating cells through differentiation therapy. Stem Cell Res 21: 117-123, 2017.
12. Li B, Gao MH, Chu XM, Teng L, Lv CY, Yang P and Yin QF: The synergistic antitumor effects of all-trans retinoic acid and C-phycocyanin on the lung cancer A549 cells in vitro and in vivo. Eur J Pharmacol 749: 107-114, 2015.
13. Greve G, Schiffmann I and Lübbert M: Epigenetic priming of non-small cell lung cancer cell lines to the antiproliferative and differentiating effects of all-trans retinoic acid. J Cancer Res Clin Oncol 141: 2171-2180, 2015.
14. Li HX, Zhao W, Shi Y, Li YN, Zhang LS, Zhang HQ and Wang D: Retinoic acid amide inhibits JAK/STAT pathway in lung cancer which leads to apoptosis. Tumour Biol 36: 8671-8678, 2015.
15. Chen D, Xie F, Sun D, Yin C, Gao J and Zhong Y: Nanomedicine-mediated combination drug therapy in tumor. Open Pharmaceutical Sci J 4: 1-10, 2017.
16. Xie FY, Xu WH, Yin C, Zhang GQ, Zhong YQ and Gao J: Nanomedicine strategies for sustained, controlled, and targeted treatment of cancer stem cells of the digestive system. World J Gastrointest Oncol 8: 735-744, 2016.
17. Gao J, Feng SS and Guo Y: Nanomedicine against multidrug resistance in cancer treatment. Nanomedicine (Lond) 7: 465-468, 2012.
18. Cristiano MC, Cosco D, Celia C, Tudose A, Mare R, Paolino D and Fresta M: Anticancer activity of all-trans retinoic acid-loaded liposomes on human thyroid carcinoma cells. Colloids Surf B Biointerfaces 150: 408-416, 2017.
19. Gao J, Xia Y, Chen H, Yu Y, Song J, Li W, Qian W, Wang H, Dai J and Guo Y: Polymer-lipid hybrid nanoparticles conjugated with anti-EGF receptor antibody for targeted drug delivery to hepatocellular carcinoma. Nanomedicine (Lond) 9: 279-293, 2014.
20. Kapoor DN, Bhatia A, Kaur R, Sharma R, Kaur G and Dhawan S: PLGA: A unique polymer for drug delivery. Ther Deliv 6: 41-58, 2015.
21. Gao J, Chen H, Song H, Su X, Niu F, Li W, Li B, Dai J, Wang H and Guo Y: Antibody-targeted immunoliposomes for cancer treatment. Mini Rev Med Chem 13: 2026-2035, 2013.
22. Gao J, Feng SS and Guo Y: Antibody engineering promotes nanomedicine for cancer treatment. Nanomedicine (Lond) 5: 1141-1145, 2010.
23. Wang J, Wu Z, Pan G, Ni J, Xie F, Jiang B, Wei L, Gao J and Zou W: Enhanced doxorubicin delivery to hepatocellular carcinoma cells via CD147 antibody-conjugated immunoliposomes. Nanomedicine 14: 1949-1691, 2018.
24. Herr JK, Smith JE, Medley CD, Shangguan D and Tan W: Aptamer-conjugated nanoparticles for selective collection and detection of cancer cells. Anal Chem 78: 2918-2924, 2006.
25. Xiao Z and Farokhzad OC: Aptamer-functionalized nanoparticles for medical applications: Challenges and opportunities. ACS Nano 6: 3670-3676, 2012.
26. Auffan M, Rose J, Bottero JY, Lowry GV, Jolivet JP and Wiesner MR: Towards a definition of inorganic nanoparticles from an environmental, health and safety perspective. Nat Nanotechnol 4: 634-641, 2009.
27. Cushing BL, Kolesnichenko VL and O'Connor CJ: Recent advances in the liquid-phase syntheses of inorganic nanoparticles. Chem Rev 104: 3893-3946, 2004.
28. Mamot C, Ritschard R, Wicki A, Stehle G, Dieterle T, Bubendorf L, Hilker C, Deuster S, Herrmann R and Rochlitz C: Tolerability, safety, pharmacokinetics, and efficacy of doxorubicin-loaded anti-EGFR immunoliposomes in advanced solid tumours: A phase 1 dose-escalation study. Lancet Oncol 13: 1234-1241, 2012.
29. Miller K, Cortes J, Hurvitz SA, Krop IE, Tripathy D, Verma S, Riahi K, Reynolds JG, Wickham TJ, Molnar I and Yardley DA: HERMIONE: A randomized Phase 2 trial of MM-302 plus trastuzumab versus chemotherapy of physician's choice plus trastuzumab in patients with previously treated, anthracycline-naïve, HER2-positive, locally advanced/metastatic breast cancer. BMC Cancer 16: 352, 2016.